OBSERVING COSMIC RAYS WITH THE HIGH RESOLUTION FLY'S EYE (HiRes) DETECTOR*

J.N. Matthews

for the HiRes Collaboration

University of Utah, Department of Physics
and
High Energy Astrophysics Institute
115 S 1400 E #201 JFB, Salt Lake City, UT 84112, USA

(Received May 6, 2004)

The High Resolution Fly's Eye (HiRes) observatory consists of two detector sites separated by 12.6 km in the western Utah desert. These sites observe Ultra High Energy Cosmic Rays (UHECR) using the air fluorescence technique. Reconstructing the data collected at these sites, we have measured the spectrum, composition, and anisotropy in arrival direction of these cosmic rays. The spectrum is measured from $\sim 10^{17}$ eV and shows significant structure including the "ankle" and a steep fall off which is consistent with a GZK threshold. The composition is measured using the $X_{\max}$ technique. It was found to be predominantly light and unchanging over the range from 10^{18} to $3{\times}10^{19}$ eV. Finally, several different styles of searches for anisotropy in the data were performed. No significant anisotropy was found.

PACS numbers: 95.85.Ry, 96.40.De, 96.40.Pq, 98.70.Sa

1. Introduction

Ultra High Energy Cosmic Rays: What are they? Where do they come from? How do they get accelerated to such high energies? Does does the spectrum end as expected? What is the physics underlying the acceleration of these particles and those portions of the universe where they are created? In resolving the riddle of Ultra High Energy Cosmic Rays (UHECR), our potential hints are few: the shape of the spectrum, the composition of the cosmic rays themselves, and point sources or anisotropy.

* Presented at the Cracow Epiphany Conference on Astroparticle Physics, Cracow, Poland, January 8–11, 2004.

The cosmic ray spectrum is steeply falling and relatively featureless. Over many orders of magnitude it follows a simple power law dependence: $E^{-2.8}$. What structure there is, presents itself near 10^{16} eV, "the knee", where the spectrum becomes slightly more steep and again at $10^{18.5}$ eV, 'the ankle", where it becomes slightly less steep.

After the discovery of the Cosmic Microwave Background (CMB) it was quickly realized that collisions between Ultra High Energy (UHE) cosmic rays and these low energy (2.7 K) photons would result in photo-pion production (via a delta resonance). This should render the universe essentially opaque to UHE cosmic rays beyond the mean free path in the CMB: approximately 100 Mpc. Therefore, we expect to observe a cut-off in the cosmic ray spectrum near 1.6×10^{19} eV. This is known as the Greisen–Zatsepin–Kuzmin (GZK) cutoff [1, 2]. Events observed above this energy must come from "nearby" sources.

In 1991, the Fly's Eye experiment unexpectedly observed an event with an amazing 3.2×10^{20} eV, well above the GZK limit. The Volcano Ranch, Haverah Park, and Yakutsk experiments each also observed one "super-GZK" event. More recently, the AGASA (Akeno Giant Air Shower Array) experiment observed a significant flux of "super-GZK" events. With a significantly higher exposure, AGASA observed ten "super-GZK" events. The flux observed above the GZK limit in these experiments appears to be inconsistent. Is this a resolution problem, an energy scale problem, or something else?

2. Detector description

The Fly's Eye and its successor the High Resolution Fly's Eye (HiRes) both use the earth's atmosphere as their calorimeter. When a cosmic ray enters the atmosphere, it collides with an air molecule. In this hard collision, many secondary particles are produced. These, in turn, go on to collisions of their own. Thus, a cascade of particles or Extensive Air Shower (EAS) potentially containing many billions of particles, results. As the charged particles of the shower pass through the atmosphere, they excite the gas. When the molecules return to their ground state, they emit fluorescence light, mostly in the ultra-violet. The fluorescence light is emitted isotropically, so that if one looks, a track glowing in the UV develops at the speed of light.

The HiRes experiment employs an array of telescopes to observe these tracks (see figure 1). Each telescope uses a 5 m^2 spherical mirror to gather light and focus it onto a 16×16 array of hexagonal PMTs in a hexagonal close-pack (AKA honeycomb) geometry. Each PMT subtends 1° of sky. The PMTs observe events though a 300–400 nm UV band-pass filter which transmits the strongest air fluorescence signals while filtering out background star and man-made light.

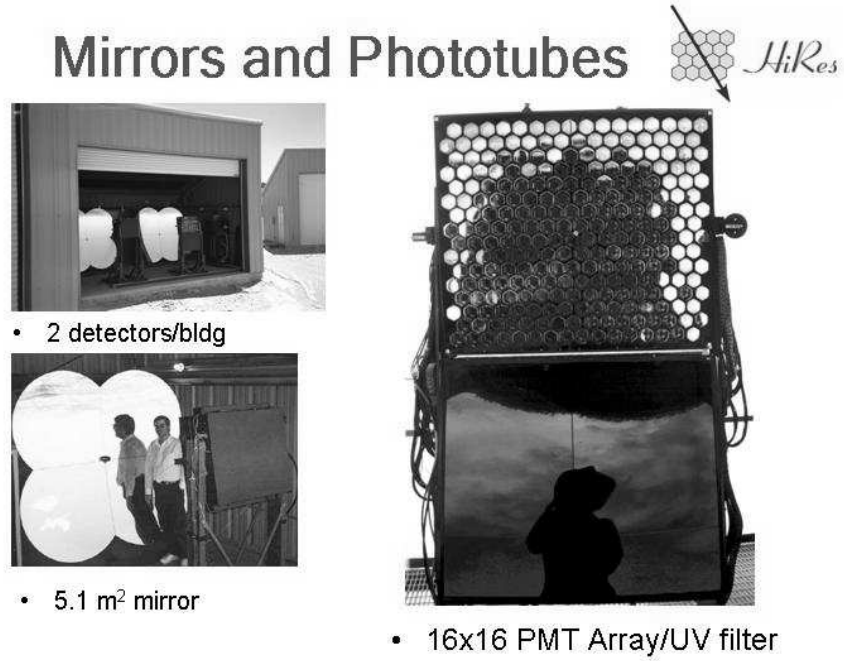

Fig. 1. Some pictures of the HiRes detectors. Top left is a typical HiRes building housing two telescopes. Bottom left, one can see a mirror in the background and a PMT array in the foreground. The front side of the PMT cluster can be seen on the right where the UV filter has been opened to show the tubes.

Like its predecessor, the High Resolution Fly's Eye is located at the US Army's Dugway Proving Ground in Utah's west desert. The observatory is composed of two detector sites separated by 12.6 km. The first site, HiRes-I, contains 22 telescopes arranged in a single ring geometry observing nearly 2π in azimuth and between 3° and 17° in elevation. Many of these telescopes were previously used in the HiRes prototype and they are instrumented with an older version sample and hold electronics. The 5.6 μs integration period of these electronics is long enough to contain signals from all reconstructible events. The current HiRes-I site became operational in the spring of 1997.

The second site, HiRes-II, is composed of 42 telescopes forming two rings. It also observes nearly 2π in azimuth, but covers a larger slice in elevation — from 3° to 31° above the horizon. HiRes-II was completed late in 1999; considerably newer, these telescopes are instrumented with 100 ns FADC electronics.

With smaller pixels and larger mirrors than the Fly's Eye, the High Resolution Fly's Eye has an order of magnitude greater aperture than the original

Fly's Eye or the AGASA ground array (1000 km^2 str vs. 100 km^2 time averaged aperture). It also has significantly improved energy and shower profile resolution.

The High Resolution Fly's Eye was designed for stereo observation of cosmic ray showers with energies above 3×10^{18} eV. The physics goals are to measure the cosmic ray spectrum and chemical composition of the incoming particles. We also search for point sources and/or anisotropy as well as Ultra High Energy neutrinos, gamma rays, and other exotic particles. For the present paper, we concentrate on the Ultra High Energy Cosmic Ray (UHECR) spectrum and composition. We also briefly touch on anisotropy and point source searches.

3. Data collection and analysis

The HiRes detector collects data on clear, moon-less nights and has a duty cycle near 10%. The current HiRes-I data set consists of events from the date of the detector's turn-on in June of 1997 through February of 2003. It contains 3600 hours of data, 2820 hours of which are 'good weather" as identified by the operators. During that time, over 125 million triggers were written, however these mostly consist of noise and atmospheric monitoring data. Amongst these, 12,709 downward track-like candidates were selected for reconstruction after cuts such as minimum track distance, minimum light level, and observation of the shower maximum.

Due to the limited angular coverage of HiRes-I, it is unable to completely reconstruct the event geometry using timing information alone. However, the HiRes Prototype, which had extensive zenith angle coverage, has previously shown that while the depth of shower maximum fluctuates, the shower shape has little variation. [3] That measurement also found that the shower profile was a good fit to a parameterization previously presented by Gaisser and Hillas. [4] Using the additional constraint of the expected shower shape allows HiRes-I data to be reconstructed with significantly smaller uncertainties. We call this a profile constrained fit. After reconstruction and cutting on minimum track length, maximum Čerenkov light contamination, 6920 showers remained.

The HiRes-II data set consists of 144.27 hours of good weather data between December 1999 and May 2000; a period where the trigger conditions were stable. The analysis for these events is similar, except that with the longer angular tracks and the improved timing resolution the events can now be reconstructed based on timing information — the profile constraint is no longer necessary. For this period, 781 events remained after cuts [5, 6].

4. Monte Carlo studies and aperture

For HiRes-I, Monte Carlo (MC) studies were performed to assess the reliability of the PCF method. The simulated events were subjected to the same selection criteria and cuts imposed on the data. Not including atmospheric fluctuations, an RMS energy resolution of better than 20% was seen above 3×10^{19} eV. However, the resolution degrades at lower energies to about 25% at 3×10^{18} eV. These MC results were cross-checked by examination of a small set of stereo events where the geometry is more precisely known. Comparing the reconstructed energies and geometric parameters using monocular and stereo geometries, we obtained resolutions in good agreement with those seen in the MC.

At HiRes-II, the longer track lengths significantly improve the situation. Not only is the profile constraint no longer necessary, but the reconstruction is more robust yielding better geometrical and energy resolution. The energy resolution determined by Monte Carlo is 16% between $10^{17.5}$ and 10^{18} eV and improves to better than 12% above 10^{19} eV. A series of energy resolution plots from the HiRes-II Monte Carlo is shown in figure 2.

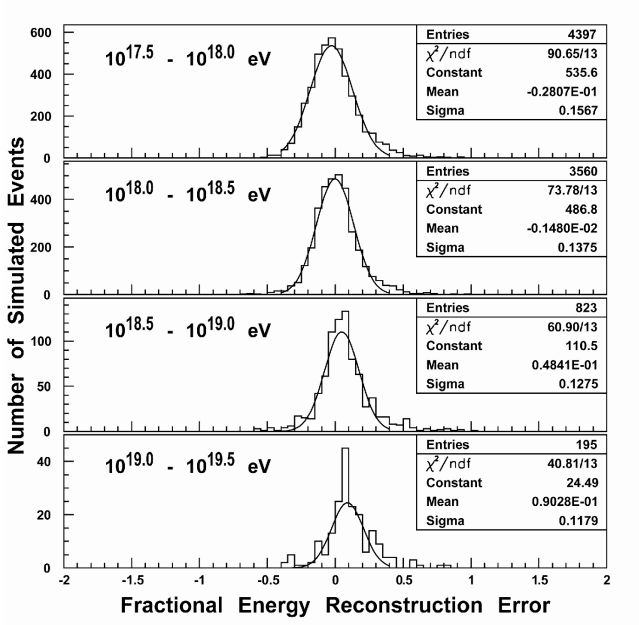

Fig. 2. The HiRes-II energy resolution shown as a function of energy. In the lowest energy slice, The energy resolution is 16% in the lowest energy slice and improves to better than 12% above 10^{19} eV.

The MC simulation is also used to calculate the detector aperture. Again, the simulated events were subjected to the same reconstruction algorithm and cuts applied to the data. To verify the reliability of this calculation, we compared, at different energies, the impact parameter ($R_{\rm p}$) and the zenith angle (θ) distributions, which define the detector aperture. The data/Monte Carlo comparison overlays for the $R_{\rm p}$ and zenith angle distributions at three energies in figure 3. The MC predictions for these are very sensitive to details of the simulation, including the detector triggering, optical ray-tracing, signal/noise, and the atmospheric modeling. There is excellent agreement between data and Monte Carlo.

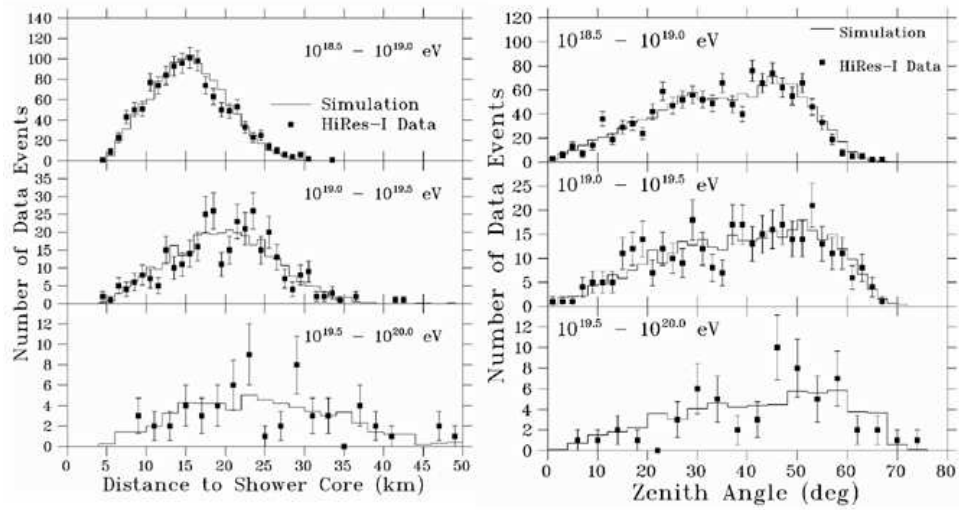

Fig. 3. Data/Monte Carlo comparisons for HiRes-I. The data is shown as points, while the Monte Carlo is represented as a histogram. The distributions are shown for the impact parameter, $R_{\rm p}$, on the left and for the zenith angle on the right. They are broken down by energy bins: (a) $10^{18.5}$, (b) $10^{19.0}$, and (c) $10^{19.5}$ eV. The MC distributions have been normalized to the number of data events.

The monocular reconstruction apertures are shown in figure 4; both HiRes-I and II approach 10^4 km^2 steradian above 10^{20} eV. We restrict our result for HiRes-I to energies $>3\times10^{18}$ eV since below this the event reconstruction technique becomes unstable. Meanwhile, the HiRes-II data set becomes statistically depleted above 10^{19} eV due to a significantly shorter running time. We deal with this problem by combining the two sets of monocular data to get one spectrum which stretches from near 10^{17} eV to beyond 10^{20} eV.

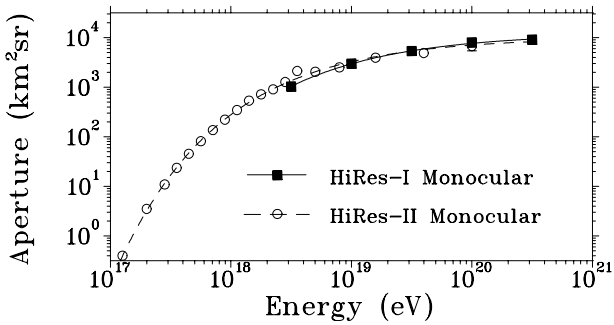

Fig. 4. Calculated HiRes monocular reconstruction aperture in the energy range 10^{17}–3×10^{20} eV. The HiRes-I and -II apertures are shown by the squares and circles, respectively.

5. The spectrum

We calculated the cosmic ray flux for HiRes-I above $3{\times}10^{18}$ eV, and for HiRes-II above $2{\times}10^{17}$ eV. This combined spectrum is shown in figure 5, where the flux, $J(E)$, has been multiplied by E^3. In the region of overlap, the HiRes-I and HiRes-II detectors are in excellent agreement. The Fly's Eye stereo spectrum (normalized down 7% in energy — which is within uncertainties) and the HiRes Prototype/MIA spectrum are overlayed for comparison. There is remarkable agreement between all spectra measured by fluorescence detectors.

Structural features are evident in the spectra. The ankle, at $\sim 10^{18.5}$ eV, in the Fly's Eye data, also shows up clearly and at the same location in the monocular HiRes data. However, where the Fly's Eye ran out of statistical power at higher energies, the HiRes data continues. There is evidence of a turn-over which is consistent with a GZK effect.

The GZK threshold is calculated for proton-photon collisions. Another piece of information one would like to have here is the composition of the incident cosmic rays. This will be addressed below.

One can ask the question, "Does the spectrum continue, unabated, with the same spectral index above the predicted GZK threshold?" To study this, we fit the spectrum to a single power law above the ankle. The slope of the spectrum in this region is 2.84 which leads us to predict that beyond $10^{19.5}$ eV we would expect to have observed 43.2 events. In this data, we have only 11 events in this energy range.

The largest systematic uncertainties are the absolute calibration of the detectors ($\pm 10\%$) [10], the yield of the fluorescence process ($\pm 10\%$) [11], the correction for unobserved energy in the shower ($\pm 5\%$) [12, 13], and the modeling of the atmosphere. [14] To test the sensitivity of the flux mea-

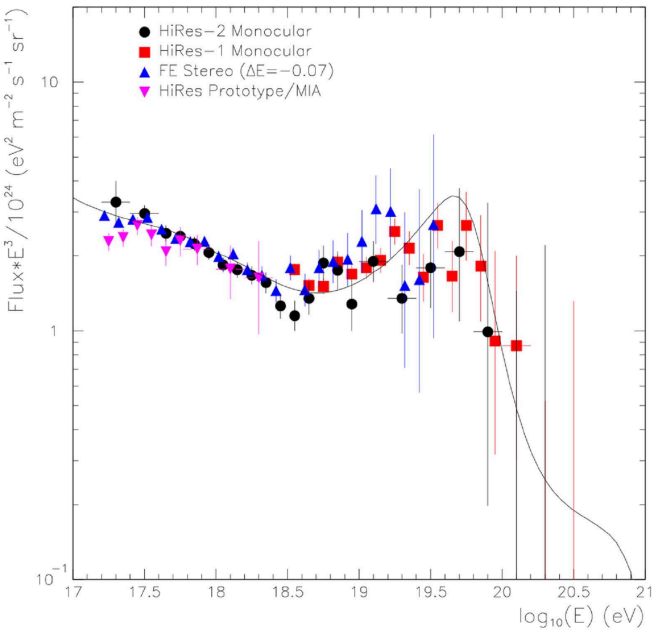

Fig. 5. The UHECR spectrum. The spectrum as measured by four independent fluorescence data sets: HiRes-I monocular HiRes-II monocular, Fly's Eye stereo (normalized down 7% in energy), and HiRes Prototype/MIA. There is remarkable agreement between the data. In this plot, the error bars represent the 68% confidence interval.

surement to atmospheric uncertainties, we generated new MC samples with atmosphere altered by ±1 RMS value. The MC was then reconstructed using the expected average atmosphere. We found a ±15% change which represents a conservative over-estimate of the one sigma uncertainty from atmospheric effects. If we add in quadrature this uncertainty to the others mentioned above, we find a net systematic uncertainty in $J(E)$ of 21%. This uncertainty is common to the fluxes for HiRes-I and HiRes-II. There is an additional relative calibration uncertainty between the two sites which is less than 10% [5].

6. Composition

A second important area of study is the composition of the UHECR's. The information aids in understanding UHECRs in general and, as mentioned above it provides critical input to verifying the GZK effect.

At HiRes, we use the $X_{\max}$ technique to determine composition. From the shower profile, we measure $X_{\max}$, the depth of shower maximum. The Monte Carlo is used to study the resolution both in $X_{\max}$ and in energy. We then compare $X_{\max}$ *versus* energy distribution of the data with predictions from CORSIKA using both the QGSjet and Sibyll hadronic generators. Finally, we measure the elongation rate or the change in $X_{\max}$ with energy, $\Delta X_{\max}/\Delta E$.

This analysis was done with a small subset of the first stereo data from HiRes. It contains approximately 800 events collected between December 1999 and September 2001. Since the data is measured in stereo, the geometry is much more precisely known and there is a second measurement of the energy. In the reconstructed Monte Carlo, we found an energy resolution of 12% and an $X_{\max}$ resolution of 27 gm/cm^2.

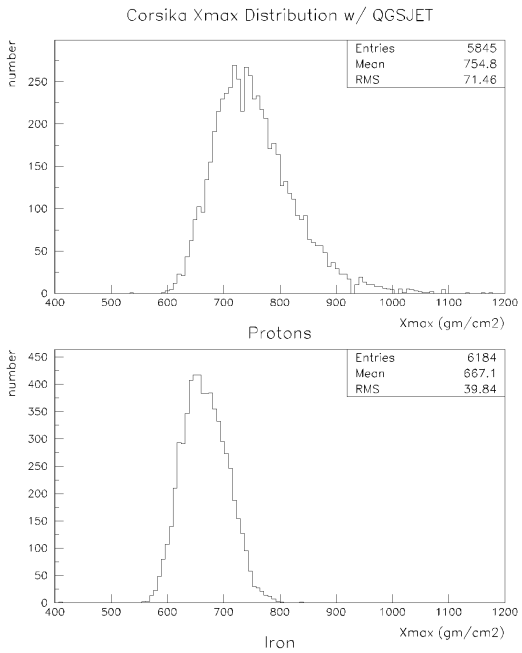

Fig. 6. The $X_{\max}$ Width Distributions for Corsika using QGSjet. The distributions reflect a spectrum of protons (above) and iron (below). The Monte Carlo $X_{\max}$ distributions for protons and iron have significant width and overlap.

From the Sibyll and QGSjet hadronic interaction models, which are built into Corsika, we expect that the depth of shower maximum should be about 100 gm/cm^2 deeper for protons than for iron at any given energy. Further, for constant composition, the elongation rate or the change in $X_{\max}$ should

be about 50 gm/cm^2 per decade in energy. The separation between the two models is of order 20 gm/cm^2 so that defines the required resolution. (These models are shown in figure 8.)

In addition to the separation in mean $X_{\max}$, the proton and iron distributions look very different. As might be expected, the iron distribution is significantly narrower than that for protons. (See figure 6.) This gives one another handle on the composition. Since the distributions overlap, composition can not be determined on an event by event basis. However, from the mean and the width of the distribution, one can make a determination for populations as a function of energy.

In figure 7, the $X_{\max}$ distribution for the data is compared to proton and iron nuclei models using the Sibyll and QGSjet hadronic models. The plot on the left (protons) is a pretty good match for the data — the data is very proton-like. The data comes much closer to matching either of the proton model curves than the iron model curves. However, the data looks as if it is shifted slightly to lower $X_{\max}$ values relative to the models. While the iron model curves are a much poorer match, they do have a clear excess on the low $X_{\max}$ end.

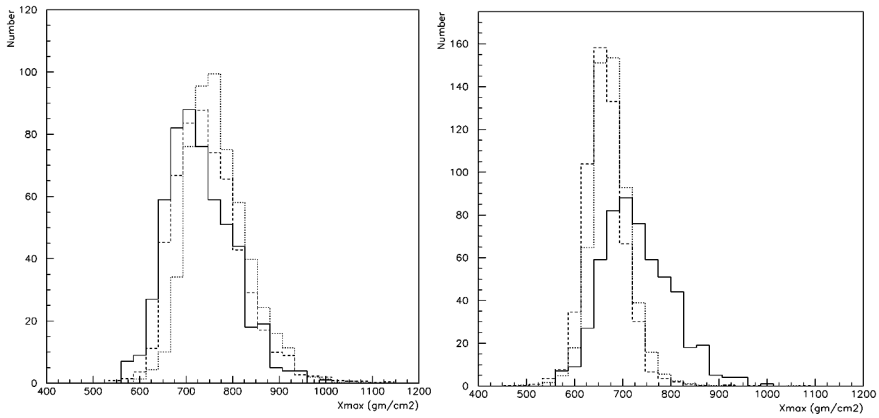

Fig. 7. Data-Monte Carlo comparisons for proton and iron nuclei models. On the left, the data (solid line) is compared to Corsika proton models using Sibyll (light dots) and QGSjet (heavy dots). On the right, the data (solid) is compared to Corsika iron models using Sibyll (light dots) and QGSjet (heavy dots). The data is clearly much more proton-like.

One can, then, construct a toy model consisting of a two elements protons and iron. Fitting the two component mixing model, for the "best" ratio of protons to iron, we find that with Sibyll our data prefers a composition which is about 60% protons, while QGSjet prefers ∼80% protons. Putting

this mix into the simulation, we now find that the data and Monte Carlo distributions for $X_{\max}$ agree well with each other.

In figure 8, the mean $X_{\max}$ is plotted as a function of energy. From this, we measure an elongation rate. In the energy region covered by this data, $1{\times}10^{18}$ to $3{\times}10^{19}$ eV, the elongation rate is 54.5 ± 6.5 (*stat*) ± 4.5 (*sys)* gm/cm^2 per decade in energy. This is significantly different from the elongation rate measured with the HiRes Prototype/MIA detectors in the energy range just below this — 10^{17} to 10^{18} eV. There, the elongation rate was found to be 93.0 ± 8.5 (*stat*) ± 10.5 (*sys)* gm/cm^2 per decade in energy. The uncertainties are significantly smaller than the proton-iron separation. In addition, the two measurements are in good agreement in the range where they overlap.

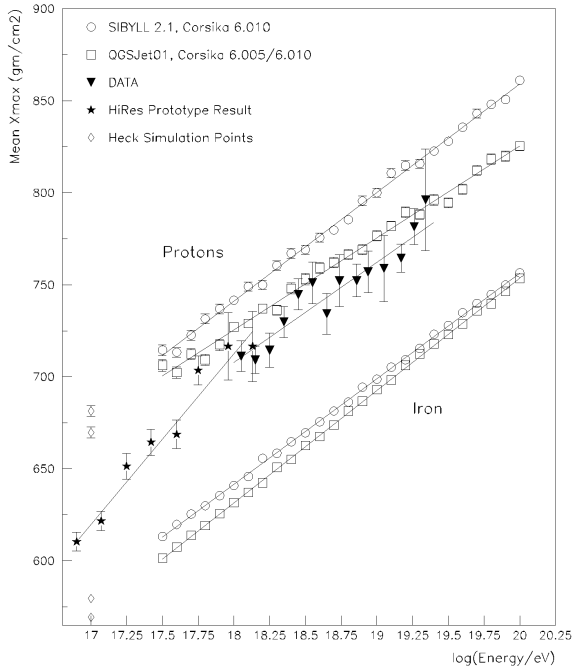

Fig. 8. The Elongation Rate. The mean $X_{\max}$ is plotted as a function of energy. The QGSjet (squares) and Sibyll (circles) hadronic models for protons and iron are also shown. For comparison, the HiRes Prototype/MIA result is also plotted.

The measurements imply that the composition starts out heavy and transitions to light in the decade between 10^{17} and 10^{18} eV. Above this, from $1{\times}10^{18}$ to $3{\times}10^{19}$ eV, the composition is light and unchanging. There are not yet enough statistics at the high end to provide significant information about the GZK region.

7. Anisotropy

Ultimately, one would also like to know the sources of the cosmic rays. Determining the type of object which is capable of accelerating particles to such high energies would provide great insight into the problem. The first step in this is looking for anisotropy in the data. The stereo data is shown in figure 9.

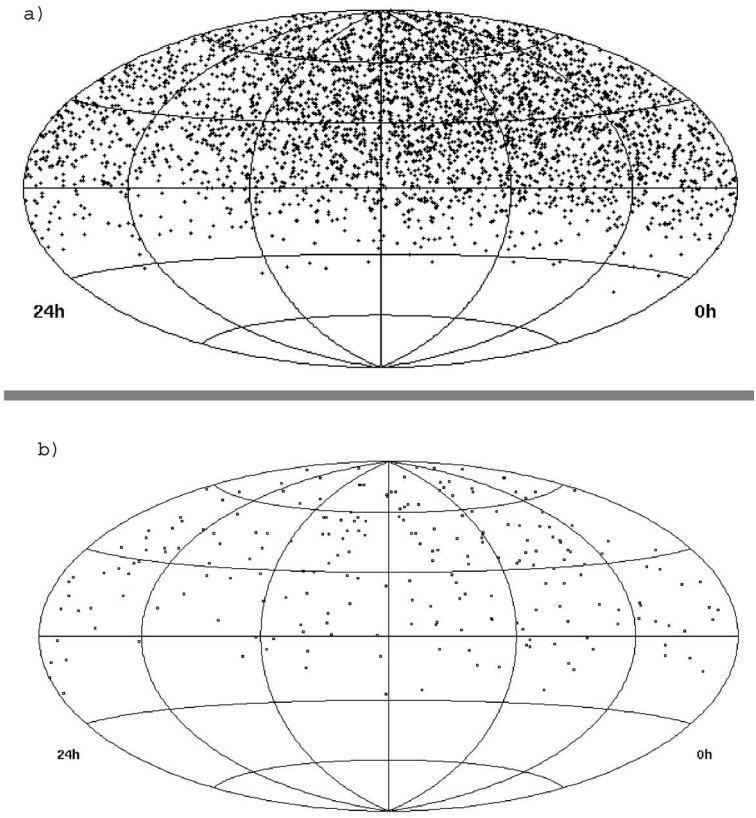

Fig. 9. Sky map of the stereo data in equatorial coordinates. Above, (a), is a map of all events collected between November 1999 and June 2003. Below, (b), is the map of well reconstructed events above 10^{19} eV. The angular resolution is better than 0.6° and the zenith angle is <70°. There are 222 events in the lower data set.

A two point correlation was performed on the data. Each event was paired with all other events. A count was performed on pairs of events separated by a given angle. The same count was performed on numerous Monte Carlo sets with the same number of events and similar exposures to

determine the uncertainties. The results can be seen in figure 10. Clustering would show up as an excess over fluctuations at small angular separations. No such signal is present. More details are presented in [17]. A similar search was performed for the monocular data [18] and it also saw no signal. Searches were also performed for a dipole moment [19] and other types of sources. We see no sign of any anisotropy and no sign of any correlation with the AGASA "doublets and/or triplet".

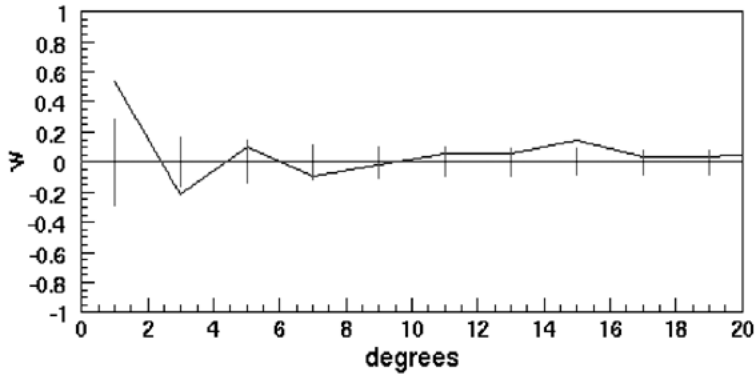

Fig. 10. The two point autocorrelation function for the stereo data. $w(\theta) = N(\theta)/N_{\rm MC}(\theta) - 1$. The error bars on the $w = 0$ line represent the size of 1σ fluctuations.

8. Conclusion

The High Resolution Fly's Eye has made measurements of the UHE cosmic ray spectrum and observes significant structure in that spectrum. In particular, it sees the ankle and a sharp decrease in the event rate at the highest energies. This is consistent with GZK cut-off expectation. It is inconsistent with the continuing spectrum which the AGASA experiment appears to observe.

Our composition measurements, from the HiRes Prototype and the current HiRes experiment indicate that the composition changes from heavy to light in the decade between 10^{17} and 10^{18} eV. Above this, from $1{\times}10^{18}$ to $3{\times}10^{19}$ eV, the composition is light and unchanging. There are not yet enough statistics at the high end to provide significant information about the GZK region.

Despite numerous efforts to find point sources or any other kind of anisotropy, the High Resolution Fly's Eye data appears to be quite isotropic so far.

The High Resolution Fly's Eye has a good amount of data under its belt. We expect to take data for five more years and significantly improve on the results presented above. Many more analyses on these and other topics are underway and will be reported on soon. As we continue to collect more data, we will revisit all of these issues as well as other topics such as neutrinos, gamma rays, *etc.*

HiRes is supported by US NSF grants PHY-9322298, PHY-9321949, PHY-9974537, PHY-9904048, PHY-0071069, PHY-0140688, PHY-0307098, by the DOE grant FG03-92ER40732, and by the Australian Research Council. We gratefully acknowledge the contributions from the technical staffs of our home institutions and the Utah Center for High Performance Computing. The cooperation of Colonels E. Fischer and G. Harter, the US Army, and the Dugway Proving Ground staff is greatly appreciated.

REFERENCES

[1] K. Greisen, *Phys. Rev. Lett.* **16**, 748 (1966).
[2] G.T. Zatsepin, V.A. K'uzmin, *Pis'ma Zh. Eksp. Teor. Fiz.* **4**, 114 (166) [*JETP Lett.* **4**, 78 (1966)].
[3] T. Abu-Zayyad *et al.*, *Astropart. Phys.* **16**,
[4] T. Gaisser, A.M. Hillas, Proc. 15th Int. Cosmic Ray.
[5] T. Abu-Zayyad *et al.*, *Phys. Rev. Lett.* **92**, 151101 (2004).
[6] T. Abu-Zayyad, *et al.*, `astro-ph/0208301`, submitted to *Astropar. Phys.*
[7] The AGASA Spectrum taken from `http://www-akeno.icrr.u-tokyo.ac.jp/AGASA/`
[8] T. Abu-Zayyad, Ph.D Thesis, University of Utah (2000).
[9] X. Zhang, Ph.D Thesis, Columbia University (2001).
[10] T. Abu-Zayyad, *et al.*, to be submitted to *Nucl. Instrum. Methods.*
[11] F. Kakimoto *et al.*, *Nucl. Instrum. Methods* **A372**, 527 (1996).
[12] C. Song, Z. Cao *et al.*, *Astropart. Phys.* **14**, 7 (2000).
[13] J. Linsley, Proc. 18th Int. Cosmic Ray Conf. (Bangalore), **12**, 135 (1983).
[14] T. Abu-Zayyad, *et al.*, in preparation, and `http://www.cosmic-ray.org/atmos/`.
[15] A.N. Bunner, Ph.D. thesis (Cornell University) (1967).
[16] M. Nagano *et al.*, *Astropart. Phys.* **20**, 293 (2003).
[17] T. Abu-Zayyad, *et al.*, `astro-ph/0404137`, submitted to *Astrophys. J. Lett.*
[18] T. Abu-Zayyad, *et al.*, `astro-ph/0404366`.
[19] T. Abu-Zayyad, *et al.*, *Astropart. Phys.* **21**, 111 (2004).
[20] B. Stokes, *et al.*, *Astropart. Phys.* **21**, 95 (2004).